Scattering Rate Calculation in Multi Valley Bands of Silicon

Research Project

Submitted to the Department of Physics in partial fulfillment of the requirements for the degree of BSc. in Physics

By Soma Bahr Tahr

Supervised by

Asst. Prof. Dr. Mowfaq Jalil Ahmed

April 2023

(بِسْمِ اللَّهِ الرَّحْمَٰنِ الرَّحِيمِ)

قَالُوا سُبْحَانَكَ لَا عِلْمَ لَنَا إِلَّا مَا عَلَّمْتَنَا ۖ إِنَّكَ أَنتَ الْعَلِيمُ الْحَكِيمُ

صَدَقَ اللهُ العَظيم

(سورة اِلبقرة- الآيه 32)

Supervisor Certificate

This research project has been written under my supervision and has been submitted for the award of the degree of BSc.in (Physics).

Signature: 

Name: Asst. Prof. Dr. Mowfaq Jalil Ahmed

Date: 2023-03-27

I confirm that all requirements have been completed.

Signature:

Name: Soma Bahr Tahr

Date :2023-03-27

Dedications

This Project is Dedicated To:

Allah Almighty, my Creator and my Master, My great teacher and messenger, Mohammed (May Allah bless and grant him), who taught us the purpose of life, My homeland Kurdistan, the warmest womb, The Salahaddin University; my second magnificent home; My great parents, who never stop giving of themselves in countless ways, My beloved brothers and sisters, To all my family, the symbol of love and giving, My friends who encourage and support me, All the people in my life who touch my heart.

ACKNOWLEDGEMENTS

First and foremost, I must acknowledge my limitless thanks to Allah, the Ever-Magnificent; the Ever-Thankful, for His help and bless. I owe a deep debt of gratitude to the physics department and Salahaddin university for giving us an opportunity to complete this work. I am very appreciative to my colleagues in the physics department. I am grateful to some people, who worked hard with me from the beginning till the completion of the present research particularly my supervisor A.Prof. Dr. Mowfaq Jalil, who has been always generous during all phases of the research. I would like to take this opportunity to say warm thanks to all my beloved friends, who have been so supportive along the way of doing my thesis. I also would like to express my wholehearted thanks to my family for the generous support they provided me throughout my entire life and particularly through the process of pursuing the thesis. Last but not least, deepest thanks go to all people who took part in making this thesis real.

Table of contents

List of Figure

List of Table

Abstract

We simulate the phonon scattering rate spectra of silicon at room temperature(300k) and liquid nitrogen (77k). The technique takes into account silicon's nonparabolic, ellipsoidal band structure of the first conduction band, as well as the effects of acoustic and intervalley phonon scattering. Using coupling factors derived from deformation potential theory and Fermi's Golden Rule, the explicit expression for intervalley phonon scattering is obtained. Deformation potentials are also used to formulate acoustic phonon scattering. Silicon has been chosen because of its importance for device applications, and is at the heart of semiconductor technology for transistors, integrated circuits, and many electronic devices. In this study multivalley model considered in order to take into account the presence of several valleys in the first conduction band of the silicon. The effects of nonparabolicity, and band anisotropy included as well. Analytical band was utilized in this project to get over difficulties caused by the detailed band structure's complexity, which is generally too hard to handle. Optical phonons are dominated scattering process in silicon and the scattering rate increase with temperature. The calculated values of scattering rate at band edge are $1.2 \times 10^{14} s^{-1}$ and $3.1 \times 10^{13} s^{-1}$ at $300k$ and $77k$, respectively.

CHAPTER ONE

Introduction to Covalent Semiconductor Band- Structure

1.1 Introduction:

The study of charge transport in semiconductors is essential for both basic physics and electronic device applications. On the one hand, transport phenomena analysis provides information about electronic interactions in crystals [1], band structure [2], lifetimes, impact ionization [3,4], and other topics. The applied aspect of the problem, on the other hand, is even more critical, because modern nanoelectronics, whose influence in all human activities appears to be growing all the time, is heavily reliant on a sophisticated understanding of many aspects of charge transport in semiconductors.

In general, charge transport is a difficult problem to solve, both mathematically and physically. Except for a few cases, the integro-differential equation that describes the problem (the Boltzmann transport equation) does not provide simple solutions.

The standard form of BTE for electron in semiconductor in the absence of magnetic field, and generation / recombination process is [5] :

$$\left(\frac{\partial f}{\partial t}\right)_{trans} + \left(\frac{\partial f}{\partial t}\right)_{diff} + \left(\frac{\partial f}{\partial t}\right)_{drift} = \left(\frac{\partial f}{\partial t}\right)_{coll} \qquad \ldots\ldots\ldots\ldots\ldots\ldots 1.1$$

Where $f \equiv f(\boldsymbol{r}, \boldsymbol{k}, t)$, is the distribution function, which is the probability density of finding the particle at time, within the infinitesimal phase space volume, centered at the phase point ($\boldsymbol{r}, \boldsymbol{k}$).

$$f(\vec{r}, \vec{k}, t) = \frac{number\ of\ occupaied\ states}{total\ number\ of\ states}$$

The terms on the left-hand side LHS of (1.1), indicate, respectively, the dependence of the distribution function on time, space, and momentum. The time

dependence (transient term) may result from oscillating external fields, whereas a space-dependence (diffusion term) of the distribution function can be caused by charge or temperature gradients, and the last term caused by applied fields (drift term). The right-hand side RHS of (1.1), is the collision term or collision integral, the collision term $\left(\frac{\partial f}{\partial t}\right)_{coll}$, accounts for all the scattering events which alter the distribution function.

Scattering process involve rapidly varying potentials that perturb the periodicity of lattice which is typically of the order of lattice constant, hence such events must be treated quantum mechanically as mentioned.

The electron scattering from an initial state (scattering -in) $|\boldsymbol{k}>$,to other empty state $|\boldsymbol{k}>$, (scattering-out) depends on three factors: the first one is the probability of finding that electron in the initial state $f(\boldsymbol{r}, \boldsymbol{k}, t)$, the second factor is the transition probability per unit time $S(\boldsymbol{k}, \boldsymbol{k}')$,that an electron with initial wave vector $\boldsymbol{k}$, scatter to the final empty state with a wave vector $\boldsymbol{k}'$, and the last factor is the probability of non-occupation for final momentum state.

Scattering mechanisms affect the nature of carrier transport and, as a result, the shapes of distribution functions [6]. The electron interacts with various scattering centers during the scattering process in crystal. In general, scattering is caused by either the intrinsic behavior of crystal-like lattice vibration or by other sources such as electrostatic fields associated with impurities [7].

Because the scattering term is independent and is considered the key to all extended transition equations, it will be treated in this project without solving the Boltzmann equation explicitly.

Chapter one introduces preliminary physical considerations as the theoretical foundation for this work. Starting with the general feature of covalent semiconductor band structure, and the band structure of silicon are briefly

discussed. A simple analytical formula for silicon's first conduction band, including first order band correction, had been expressed. The associated quantities with analytical bands, such as density of state, density of state effective mass, and conductivity effective mass, were derived in detail using the standard analytical approach. The treatments and discussions have been limited to electron motion and its interactions with lattice vibration in nonpolar semiconductors. Before qualifying on the total scattering rate, the most important scattering in silicon, lattice vibration, was briefly discussed in chapter two. Master equations for calculating the scattering rate and results are given in chapter three.

1.2 Basic Properties of Diamond Structure

Silicon has the diamond cubic crystal structure with a lattice parameter a_0 of 0.543 nm. The nearest neighbor distance is $0.235\ nm$. The diamond cubic crystal structure has an FCC lattice with a basis of two silicon atoms. The structure depicted in Figure 1.1 consists of two basis atoms and may be thought of as two inter-penetrating face cantered cubic (FCC) lattices, one displaced from the other by a translation $\frac{a_\circ}{4}(1,1,1)$ of along a body diagonal.

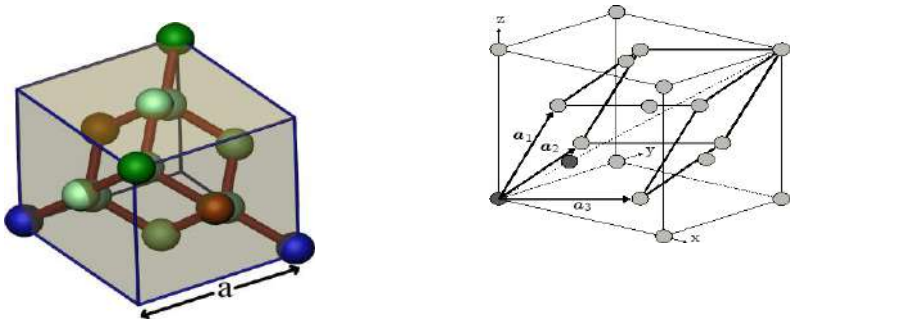

[a] [b]

Figure 1.1: *(a) Crystallographic unit cell (unit cube) of the diamond structure. (b) The primitive basis vectors of the face cantered cubic (FCC) lattice and the two atoms forming the basis are highlighted.*

In cubic semiconductors such as Si or Ge the two atoms of the basis are identical and the structure is called the diamond structure. If the two basis atoms are different, the structure is called the zinc-blende structure. Many III-V semiconductors such as GaAs, InAs, or InP are of zinc-blende type.

The translation vector, define the distance vectors that all atoms in the cluster are translated through to form another cluster in the solid, is given by

$$\boldsymbol{R} = n_1\boldsymbol{a_1} + n_2\boldsymbol{a_2} + n_3\boldsymbol{a_3} \qquad \text{……(1.2)}$$

and the reciprocal lattice vector is

$$\boldsymbol{G} = h\boldsymbol{b_1} + k\boldsymbol{b_2} + l\boldsymbol{b_3} \qquad \text{…….(1.3)}$$

In which $(n_1, n_2, n_3) and\ (\ h, k, l)$ are integers.

1.3 Brillouin Zone of Silicon

The first Brillouin zone (BZ) represents the central (Wigner-Seitz) cell of the reciprocal lattice. It contains all points nearest to the enclosed reciprocal lattice point. The boundaries of the first BZ are determined by planes which are perpendicular to the reciprocal lattice vectors pointing from the center of the cell to the lattice points nearest to the origin of the cell at their midpoints. For silicon, reciprocal lattice vectors correspond to a body cantered cubic (bcc) lattice in the reciprocal space. The Wigner-Seitz cell of this BCC lattice is the first Brillouin zone (BZ). This primitive unit cell reflects the full symmetry of the lattice and is equivalent to the cell obtained by taking all points that are closer to the center of the cell than to any other lattice point. The first Brillouin zone has the shape of a truncated octahedron. It can be visualized as a set of eight hexagonal planes halfway between the center of the cell and the lattice points at the corner, and six

square planes halfway to the lattice points in the center of the next cell, figure (1.2a) . [8]

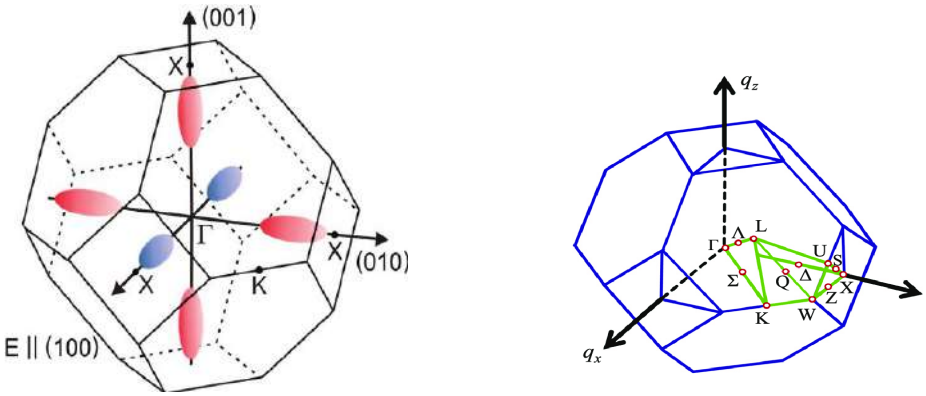

[a] [b]

Figure 1.2: *(a) First Brillouin zone of the FCC lattice. (b) The inset gives the locations of certain symmetry points and symmetry lines in the BZ.[8]*

Table1.1: *Summary of the symmetry points and directions in the brillouin zone [9]*

Symmetric Points/		
Directions	Coordinate	Remark
Γ	$(0,0,0)$	Origin of k space
X	$(1,0,0)$	Middle of square faces
L	$(\frac{1}{2},\frac{1}{2},\frac{1}{2})$	Middle of hexagonal faces
K	$(\frac{3}{4},\frac{3}{4},\frac{3}{4})$	Middle of edge shared by two hexagons
U		Middle of edge shared by a hexagons and a square
W		Middle of edge shared by two hexagons and a square
Δ	$\langle 1,0,0\rangle$	Directed from Γ to X
Λ	$\langle 1,1,1\rangle$	Directed from Γ to L
Σ	$\langle 1,1,0\rangle$	Directed from Γ to K

The Brillouin zone with the points and directions of high-symmetry marked using Greek letters and Roman letters for points on the surface [9] , figure 1.2b .

Table 1.1 summarizes these symmetry points and directions. These points and directions are of importance for interpreting the band structure plots.

1.4 Band structure of silicon

The electronic band structure of a solid describes the range of energy levels that electrons may have within it, as well as the ranges of energy that they may not have (called band gaps or forbidden bands). The lower conduction bands (at the top of the figure) and the upper valence bands of silicon are shown in fig. (1.3). The band gap extends from the top of the valence band at the point to the bottom of the conduction band near the point [10] . Within the gap, no propagating, wave-like states exist, so that optical transitions from conduction to valence band must have an energy greater than the band gap. Similarly, optical absorption occurs when the photon energy is larger than the band gap. Now, we notice that, at the point labeled, the lowest conduction connects to a second conduction band. From detailed transport simulations, it is now thought that these low energy photons are coming from optical transitions from the second conduction band to the first conduction band near, which is a totally unexpected result. Thus, it is clear that the carriers are getting distributed through large regions of the Brillouin zone, and exist in a great many bands, rather than merely staying around the minima of the conduction band. Thus, the transport itself becomes even more complicated in some sense, if we are to clearly study the detailed physics of scattering in semiconductors and in semiconductor devices. In using the full band structure, e.g., the coupling strength for the electron–phonon interaction can be determined throughout the Brillouin zone, and varies with the momentum state (that is, where the electron actually sits in the Brillouin zone). Approaches, upon the initial and final momentum states such as the cellular Monte Carlo. take into account this

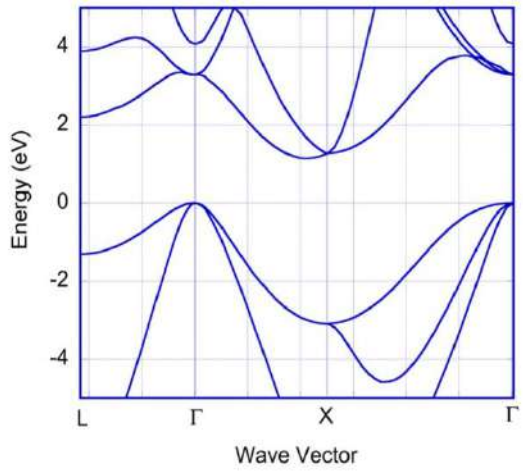

Figure 1.3: *The band structure of Si, computed with an empirical pseudo-potential method. The band gap exists in the region from 0 to 1.2 eV, where no wave states exist.[11]*

momentum dependent coupling strength to improve the Monte Carlo approach. Today, such full-band Monte Carlo simulation approaches are available in many universities, as well as from a number of commercial vendors. However, one must still be somewhat careful, as not all full-band approaches are equal and not all Monte Carlo approaches are equivalent. This extends to the band structure, the nature of the lattice vibrations, the details of the electron–phonon interactions, and the details of the transport physics and the methodology by which this physics is incorporated within the code. One cannot simply acquire a code and use it to get meaningful results without understanding its assumptions and its limitations.

1.4.1 The General Feature of Covalent Semiconductor Band- Structure

Energy band structure is constructed by calculating the allowed energy eigenvalues against the wave vector along different crystallographic directions. To simplified the basic feature of the band structure of covalent semiconductors of group four, one can concern the general model. Such model consists of one conduction band with three-valiance bands, as illustrated in figure 1.4. The minima of conduction band located at Γ point where ($\boldsymbol{k} = 0$) at L point where ($\boldsymbol{k} = \frac{\pi}{a_\circ}, \frac{\pi}{a_\circ}, \frac{\pi}{a_\circ}$), here being the lattice parameter, and along Δ lines $\boldsymbol{k}$=(k,0,0). The topes of valance band are located at Γ point [12] . The band gap becomes direct if the conduction band minima located at Γ point (which is the same reference

point that represents the top of valance band), otherwise the band gap is indirect i.e., when the location of the first conduction band minima at some point except the central point Γ.

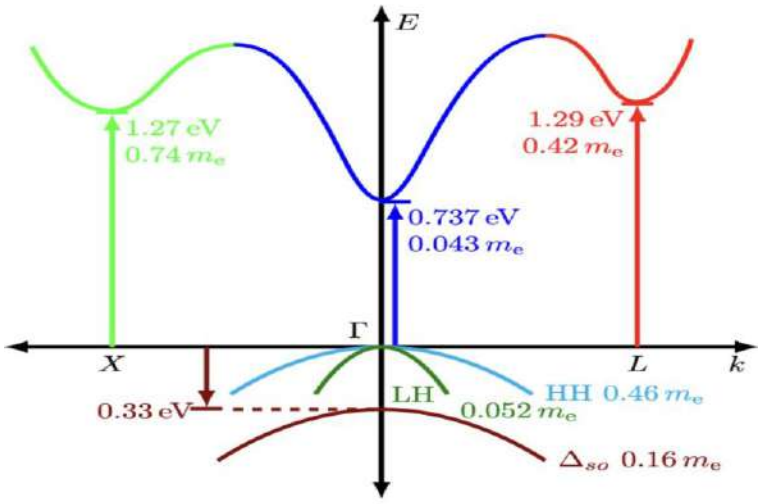

Figure 1.4: *The general model of semiconductor band structure.*

This work focuses on the first conduction band only. For such study the electrons which contribute to charge transport, even at high fields, are those in the six equivalent valleys along the direction, at about 85% from center of the Brillion zone. The contribution of other secondary minima neglects because of small density of state effective mass.

The actual energy-wave vector relationship for full band structure is quite complicated. Figure 1.5, shows multiple conduction bands. In addition, crossings among these bands make the identification of individual bands somewhat ambiguous, on other hand a full band structure approach is time consuming procedure, for that reason it is out of this calculation. In terms of electron transport in semiconductors, it is usually too difficult to deal with the complication of the detailed band structure, hence analytical band becomes candidate to overcome such difficulties. In these models, the energy-wave vector relation expressed analytically with adjustable parameters to capture some features of the full band structure without losing the credibility. There are usually two levels of

approximation used in this case, simply parabolic, and non-parabolic bands. For the second level a correction included for higher order effects in the dispersion relationship.

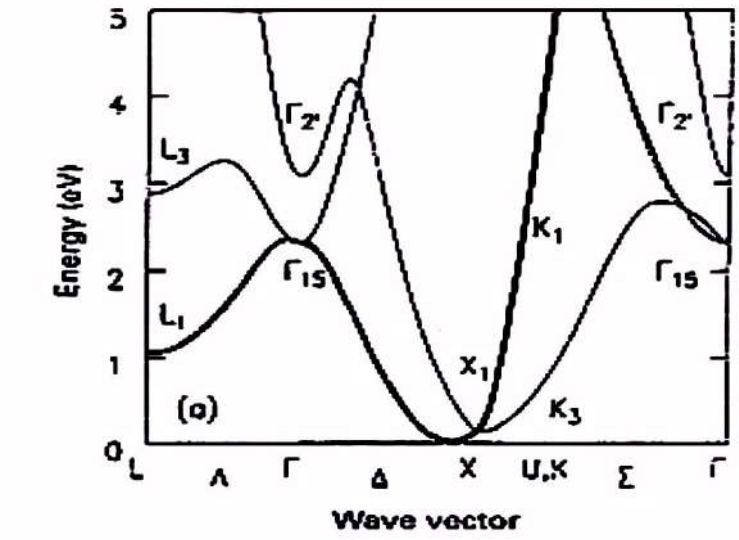

Figure 1.5: *Conduction band structure of silicon. The dark solid line is the first conduction band.*

1.4.2 Parabolic Band

For parabolic spherical (isotropic) band, the energy-wave vector relation is quadratic:

$$\varepsilon(\boldsymbol{k}) = \frac{\hbar^2 k^2}{2m^*} \qquad \text{.....(1.4)}$$

Where m^*, is the effective electron mass at the conduction band minimum.

For such bands the electron energy proportional linearly with square wave-vector.

1.4.3 Non-Parabolic Band

For values of wave vector, far from the minima of conduction band; the simple relationship between the energy and wave vector cannot be valid, and the non-parabolicity occurs. For electrons in conduction band, a simple analytical way of introducing the non-parabolicity is to consider an energy-wave vector relation of type,

$$\gamma(\varepsilon) = \varepsilon(1 + \alpha\varepsilon) = \gamma(\boldsymbol{k}) = \frac{\hbar^2 k^2}{2m^*} \qquad \ldots\ldots\ldots\ldots\ldots\ldots(1.5)$$

Where the coefficient of non-parabolicity, and has the dimensions of an inverse energy.

The nonparabolicity factor, related to other band quantities or simply given as reciprocal of band gap. In cases the non-parabolicity factor related to admixture of conduction band states, and valance band states, is given by:

$$\alpha = \frac{\left(1+\frac{m^*}{m_\circ}\right)^2}{\varepsilon_g} \qquad \ldots\ldots\ldots\ldots\ldots\ldots(1.6)$$

Where $m_\circ$, the electron is mass in vacuum, and ε_g is the energy gap, hence, smaller bandgap materials have stronger mixing of CB, and VB states, therefore a stronger nonparabolicity. When (1.6) is applied to silicon, where $m^* \cong 0.26m_\circ$, and $\varepsilon_\circ \cong 1.12ev$, therefore α, is around $0.47ev$. For case of this study the value of α is $0.5ev^{-1}$. [ ]

For parabolic band one can substitute (α=0) in equations (1.5) and (1.6) so,

$m_c = m^*$.

1.4.4 Ellipsoidal Bands

In the treatment of spherical energy surfaces it was found that the matrix element was independent of the direction in momentum space and was independent of the wave vector (in the equipartition limit). In a many-valley semiconductor, such as

the conduction band of silicon or germanium, this is no longer the case. Because the constant energy surfaces are ellipsoidal, shear strains as well as dilational strains can produce deformation potentials. The shear strain still leads to a term that depends on the vector direction of q, and it should be expected that band edge shifts will depend on all six components of the shear tensor. Thus, there might be as many as six deformation potentials. However, in the semiconductors of interest, such as Si and Ge, the valleys are ellipsoidal and cantered on the high symmetry $< 100 >$ and $< 111 >$ axes, see figure 1.6, so that the symmetry properties allow a reduction to just two independent potentials. These are the dilational potential E_d and the uniaxial shear potential.

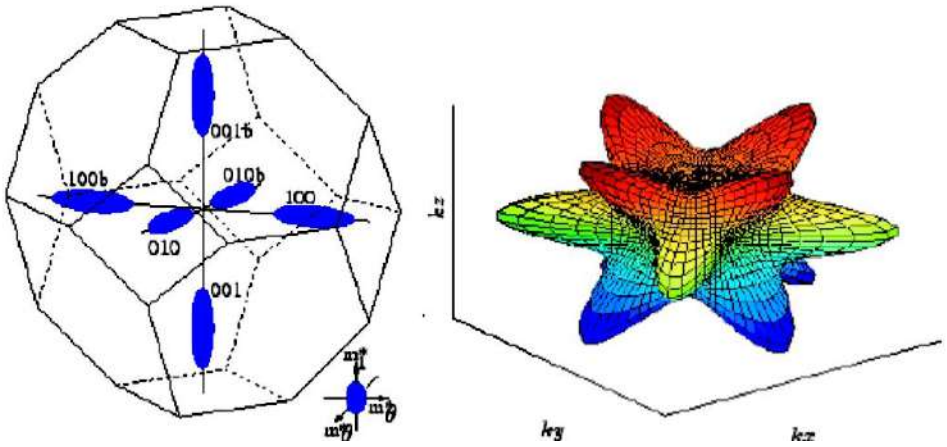

[a] **[b]**

Figure 1.6: *Constant energy surface for unstrained Si. (a) Six-fold degenerate conduction band valleys located along the directions Δ. (b) Equi-energy surface of the heavy-hole valence band.*

It should be remarked that both transverse modes are incorporated here in the general treatment. The differences above lead to different scattering rates for each principal axis within a single ellipsoidal valley. The summation over the multiple valleys (for the current) returns the overall system to cubic symmetry (unless the valleys are taken out of equilibration with each other).

1.5 Density of States and Effective Masses of Electron

The energy distribution of states, or density of states DOS, is an essential component in determining the macroscopic properties of semiconductors, such as carrier distribution, concentrations, velocity, average energy, and mobility, etc., because it is contains integrated information over the analytical band structure .In principle, when the average of specific coefficient been calculate; the contribution from each occupied states have to be added (integrated) over a range of energy, however, to do so, first one need to know the DOS in energy space. The density of states in wave vector space per unit volume of the crystal is constant, and it is equal to$\frac{1}{(2\pi)^3}$. In the reason of that each state can occupied two electrons with opposite spin, this number will be doubled. The number of states *dh* , in an element of volume $d\boldsymbol{k}$ in the wave vector space per unit volume of crystal is:

$$dh = \frac{2}{(2\pi)^3} d\boldsymbol{k} = \frac{1}{4\pi^3} d\boldsymbol{k} \qquad \text{……(1.7)}$$

the DOS in the energy space, in general, is not constant as in the case of wave vector space. For nonparabolic band

$$h(\varepsilon) = \frac{1}{2\pi^2\hbar^3} \times (2m^*)^{\frac{3}{2}} \gamma(\varepsilon)^{\frac{1}{2}} \gamma'(\varepsilon) \qquad \text{……(1.8)}$$

where $\gamma(\varepsilon)$ is given by equation (1.5) and $\gamma'(\varepsilon)$ is the first derivation of $\gamma(\varepsilon)$ respect to ε.

Since we concern with ellipsoidal / nonparabolicity band structure, as the case of this study, equation (1.8) also used for DOS of such case, but properly defined effective mass has to be used. For nonparabolicity band, one can use the Kan dispersion law (1.5), so equation (1.8), written as:

$$h(\varepsilon) = \frac{1}{2\pi^2\hbar^3} \left[2\left(m_x m_y m_z\right)^{\frac{1}{3}}\right]^{\frac{3}{2}} \gamma(\varepsilon)^{\frac{1}{2}} \gamma'(\varepsilon) \qquad \text{……..(1.9)}$$

effective mass for density of state for ellipsoidal constant energy surface can be expressed as:

$$m_D = (m_x m_y m_z)^{\frac{1}{3}} \qquad \text{.....(1.10)}$$

Equation(1.10) applied for single band minima. Nevertheless, most semiconductors have one band minimum at $\boldsymbol{k}$=*zero* as well as several equivalent anisotropic band minima at $\boldsymbol{k} \neq zero$. The effective mass of these anisotropic minima is characterized by a longitudinal mass along the corresponding equivalent direction, and two equal transverse masses in the plane perpendicular to the longitudinal direction, hence, density of state DOS is given by well known form

$$h(\varepsilon) = \frac{\sqrt{2}}{\pi^2 \hbar^2} (m_t^2 m_l)^2 \gamma(\varepsilon)^{\frac{1}{2}} \gamma'(\varepsilon) \qquad \text{.....(1.11)}$$

So, the effective mass for density of states is:

$$m^* = m_D = (m_l m_t^2)^{\frac{1}{2}} \qquad \text{.....(1.12)}$$

For silicon, $m_l = 0.98 m_\circ$ and $m_t = 0.19 m_\circ$, hence:

$$m^* = (0.98 \times 0.19^2)^{\frac{1}{3}} m_\circ \cong 0.32 m_\circ$$

CHAPTER TWO
SCATTERING PROSSES IN SILICON

2.1 Introduction

When lattice atoms vibrate around it is equilibrium position it is exciting phonons, these phonons create from the collection motion of atoms, and can interact with electron as particles obeying the principles of conservation energy, and momentum. Phonons can scatter through several mechanisms as they travel through the material. These scattering mechanisms are: Umklapp phonon-phonon scattering, phonon-impurity scattering, phonon-electron scattering, and phonon-boundary scattering. Each scattering mechanism can be characterized by a relaxation rate $\frac{1}{\tau}$ which is the inverse of the corresponding relaxation time. Because of much of scattering in semiconductors is due to lattice vibration, hence it is convenient to describe some of it is basic properties. Interest semiconductors such as silicon, has dual periodicity lattice. There are two types of scattering phonon with electron such as acoustic and optical scattering.

2.2 Acoustic Scattering

One of the most common phonons scattering processes is the interaction of the electrons with the acoustic modes of the lattice through a deformation potential. If the neighboring atom vibrates in phase, the phonon corresponding to this motion called acoustic phonons. Here, a long-wavelength acoustic wave moving through the lattice can cause a local strain in the crystal that perturbs the energy bands due to the lattice distortion. This change in the bands produces a weak scattering potential, which leads to a perturbing energy.

$$\delta(E) = \Xi_1 \Delta = \Xi_1 \nabla . \boldsymbol{u}_q \qquad \text{.....(2.1)}$$

Where Ξ_1 is the deformation potential for a particular band and Δ is the dilation of the lattice produced by a wave, whose Fourier coefficient is $\boldsymbol{u}_q$. We note here that any static displacement of the lattice is a displacement of the crystal as a whole and does not contribute, so that it is the wave-like variation of the amplitude within the crystal that produces the local strain in the bands. This variation is represented by the dilation, which is just the desired divergence of the wave. Because the divergence operator produces a factor proportional to q in the polarization direction (along the direction of propagation), only the longitudinal acoustic modes couple to the carriers in a spherically symmetry band (the case of ellipsoidal bands will be treated later). The fact that the resulting interaction potential is now proportional to q (i.e., first order in the phonon wave vector) and leads to this term being called a first-order interaction. The matrix element may now be calculated by considering the proper sum over both the lattice and the electronic wave functions.

One thing that should be recalled is that the acoustic modes have very low energy. The phonon dispersion curve for typical semiconductor shown in fig.(1.4), which is similar to dispersion curve of silicon that illustrated in same figure. It is noted from this curve that for small wave number $|\boldsymbol{q}|$, the dispersion relation for acoustic phonons apparent liner and the corresponding energy is small. When an electron will interact with a low energy phonon, it is assumed that the event happens in the same valley. This type of interaction named by intravalley acoustic scattering and its assumed elastic If the velocity of sound is $5\times 10^5 \frac{cm}{s}$, a wave vector corresponding to 25% of the zone edge yields an energy only of the order of 10meV. This is a very large wave vector, so for most practical cases the acoustic mode energy will be less than a millivolt. This will be important later when this matrix element is introduced into the scattering formulas above. Scattering processes in which the phonon energies are small and may be ignored

are termed elastic scattering events. Spherical energy surface and parabolic bands:

$$\Gamma(k) = \frac{E_1^2 k_B T}{2\pi\rho_m v_s^2 \hbar^4} E^{\frac{1}{2}} \qquad \ldots\ldots\ldots\ldots\ldots\ldots(2.2)$$

2.3 Non-Polar Optical Scattering

The vibration in opposite phase induced optical phonons. In the tetrahedrally coordinated semiconductors, there are two atoms per unit cell site and optical mode vibrations are allowed, where the two atoms vibrate relative to each other. These phonons are rather energetic, being of the order of to (or more) in energy, and lead to inelastic scattering processes, since there is a significant gain or loss of energy by the carrier during the scattering process. The importance of the inelastic scattering processes is quite clear, since the previous processes were essentially elastic. Hence, we need the optical phonons to relax the energy that is obtained from the electric field. We now want to turn to the details of these inelastic processes. Although one normally thinks of scattering occurring just within a single minimum, or valley, of the band, these optical phonons can also cause inter-valley or inter-band scattering. Such examples are scattering from the light-hole valence band to the heavy-hole valence band by a mid-zone phonon near the Γ point, or a Γ-to-L valley scattering in the conduction band by a zone-edge optical (or high-energy acoustic) phonon. The phonon dispersion curve for typical semiconductor shown in figure 1.4, which is similar to dispersion curve of silicon that illustrated in same figure. when the electron interact with higher energy phonon such that the electron transferred to other valley, then the interaction named by intervalley optical scattering and treated as inelastic mechanism.

2.4 Intervalley Phonon Scattering

An electron can be scattered from one valley to another one both by acoustical and optical phonons. Intervalley scattering can be treated as a deformation-potential interaction in the same way as intravalley scattering by optical phonons. For optical phonon, the dispersion relation, see fig.2.1 shown a little variation with phonon wave number, similarly to above analysis, if the final state of interact electron lies in the same valley, then the scattering of type intravalley, oppositely, if the final state of electron lies in deferent valley, then the scattering of type

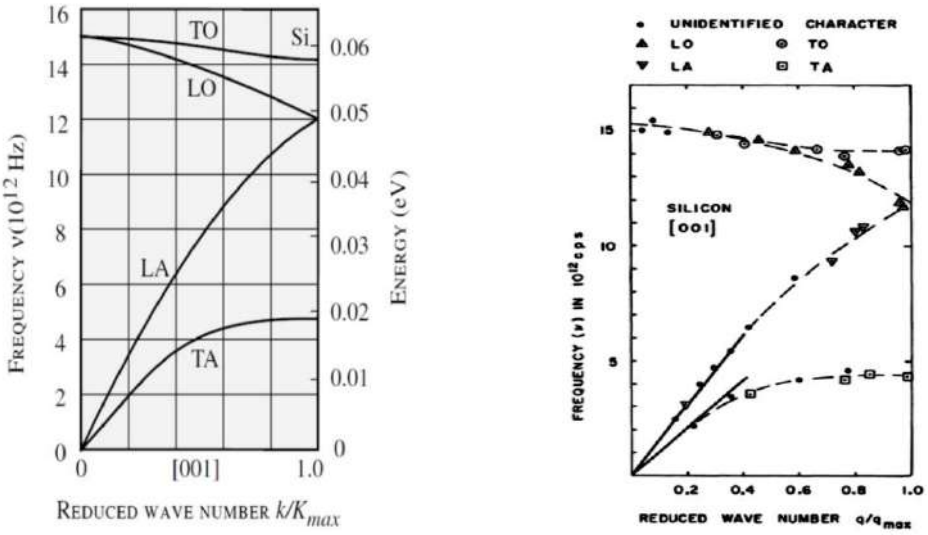

[a] [b]

Figure 2.1*: Dispersion curves of lattice vibrations for,(a) typical semiconductor, and (b) for silicon TA, LA, are transverse, longitudinal acoustic phonons, and LO, TO, are the transverse, longitudinal optical phonons respectively.*

intervalley. The associated energy with intervalley phonons is comparable with electron energy; hence the mechanism is inelastic. This type of phonons plays a dominant rule for scattering process in silicon. The number of phonons at equilibrium N_q, at a given temperature T, with quantized energy $\hbar w$, can be accounted by using Bose -Einstein statistic [7]

$$N_q = \frac{1}{e^{\frac{\hbar w}{K_B T}-1}} \quad \text{..... (2.3)}$$

$$N_q = \frac{K_B T}{\hbar w} \quad \text{..... (2.4)}$$

Among the electron phonon interaction, the phonon created (emission process) and annulated (absorption process), and for any interaction the momentum, and energy of interacted particles must be conserved. If the electron is initially at state with wave vector **k**, and kinetic energy $\varepsilon(\boldsymbol{k})$, after interaction the electron rich state with a wave vector $\boldsymbol{k'}$, and final energy $\varepsilon(\boldsymbol{k'})$. The conservation rules for energy and momentum written as:

$\varepsilon(\boldsymbol{k'}) = \varepsilon(\boldsymbol{k}) + \hbar w$ *absorption* .....(2.5)

$\varepsilon(\boldsymbol{k'}) = \varepsilon(\boldsymbol{k}) - \hbar w$ *emission* .....(2.6)

$\boldsymbol{q} = \boldsymbol{k'} - \boldsymbol{k} + \boldsymbol{G}$ *absorption* .....(2.7)

$\boldsymbol{q} = \boldsymbol{k} - \boldsymbol{k'} + \boldsymbol{G}$ *emission* .....(2.8)

Where **G**, is reciprocal lattice vector. Recalling that the phonon emission does not occur unless the initial electron energy exceeds the specified phonon energy. For this reason, the calculations which related to intervalley scattering must be taken with care below the threshold energies.

2.4.1 Equivalent X-X Intervalley Scattering

This scattering process is subdivided into $f - type$ and $g - type$ processes. A process is referred to as $f - type$, if the initial and final orientations are different, otherwise as $g - type$ process. The transition probability of this mechanism is

$$\lambda = Z_f \frac{\pi D_{XX}^2}{\rho w_{XX}} \left(N_{XX} + \frac{1}{2} \mp \frac{1}{2} \right) gx(\epsilon f) \quad \text{.....(2.9)}$$

Where ε_f is:

$$\varepsilon_f = \varepsilon_i \mp \hbar w_{XX} \quad \text{.....(2.10)}$$

N_{XX} is the equilibrium phonon number of the involved phonon type:

$$N_{XX} = \frac{1}{e^{\left(\frac{\hbar w_{XX}}{K_B T_L}\right)} - 1} \quad \text{.....(2.11)}$$

Z_f is the number of possible equivalent final valleys of the same type. For $f - type$ scattering $Z_f = 4$and for $g - type$ scattering $Z_f = 1$,D_{XX} the coupling constant, $\hbar w_{XX}$ is the corresponding phonon energy. The numerical values of the coupling constants and phonon energies are shown in Table 2.1.

Table2.1: *Numerical values for the intervalley X-X scattering rate*.

	Silicon	Germanium
$D_{XX}^{g_1}$	0.5×10^8 eV/cm	0.488×10^8 eV/cm
$\hbar\omega_{XX}^{g_1}$	0.01206 eV	0.005606 eV
$D_{XX}^{g_2}$	0.8×10^8 eV/cm	0.79×10^8 eV/cm
$\hbar\omega_{XX}^{g_2}$	0.01853 eV	0.00861 eV
$D_{XX}^{g_3}$	1.1×10^9 eV/cm	9.5×10^8 eV/cm
$\hbar\omega_{XX}^{g_3}$	0.06204 eV	0.03704 eV
$D_{XX}^{f_1}$	0.3×10^8 eV/cm	0.283×10^8 eV/cm
$\hbar\omega_{XX}^{f_1}$	0.01896 eV	0.00992 eV
$D_{XX}^{f_2}$	2.0×10^8 eV/cm	1.94×10^8 eV/cm
$\hbar\omega_{XX}^{f_2}$	0.04739 eV	0.02803 eV
$D_{XX}^{f_3}$	2.0×10^8 eV/cm	1.69×10^8 eV/cm
$\hbar\omega_{XX}^{f_3}$	0.05903 eV	0.03278 eV

2.4.2 Equivalent L-L Intervalley Scattering

For this type of scattering there is no separation into $f-$ and $g-type$ processes. The scattering rate is given as [13] :

$$\lambda(\epsilon_i) = Z_L \frac{\pi D_{LL}^2}{\rho w LL}\left(N_{LL} + \frac{1}{2} \mp \frac{1}{2}\right) gL(\epsilon_f) \qquad \text{.....(2.12)}$$

Where ϵ_f is:

$$\epsilon_f = \epsilon_i \mp \hbar w_{LL} \qquad \text{.....(2,13)}$$

N_{LL} is the equilibrium phonon number of the involved phonon type:

$$N_{LL} = \frac{1}{e^{\left(\frac{\hbar wLL}{k_B T_L}\right)} - 1} \qquad \text{.....(2.14)}$$

$Z_L = \frac{7}{2}$ for the transition between two different orientations and $Z_L = \frac{1}{2}$ for scattering within the same orientation, D_{LL} denotes the corresponding coupling constant and $\hbar w_{LL}$ is the energy of the phonon involved in the scattering process.

The numerical values of the coupling constants and phonon energies for this type of scattering are shown in Table 2.2.

Table 2.2: *Numerical values for the intervalley L-L scattering rate.[13]*

	Silicon	Germanium
D_{LL}	5.26×10^8 eV/cm	3.0×10^8 eV/cm
$\hbar\omega_{LL}$	0.02395 eV	0.02756 eV

2.4.3 Non-Equivalent Intervalley Scattering

This process involves transitions between all possible valleys in the conduction band. The scattering rate is given by [13] :

$$\lambda(\epsilon_i) = Z_j \frac{\pi D_{ij}^2}{\rho w i j}\left(N_{ij} + \frac{1}{2} \mp \frac{1}{2}\right) g_j(\epsilon_f) \qquad \text{.....(2.15)}$$

Where ϵ_f is:

$$\epsilon_f = \epsilon_i \mp \hbar w_{ij} - \Delta\varepsilon_{ij} \qquad \text{.....(2.16)}$$

N_{ij} is the equilibrium phonon number of the involved phonon type:

$$N_{ij} = \frac{1}{e^{\left(\frac{\hbar w_{ij}}{k_B T_L}\right)} - 1} \qquad \text{.....(2.17)}$$

and $\delta\epsilon_{ij}$ is given as:

$$\Delta\epsilon_{ij} = \epsilon_{j,min} - \epsilon_{i,min} \qquad \text{.....(2.18)}$$

Indices i and j stand for the initial and final valley, respectively, Z_j is the number of possible equivalent final valleys, D_{ij} is the corresponding coupling constant, $\hbar w_{ij}$ is the respective phonon energy, $\epsilon_{i,min}$ and $\epsilon_{j,min}$ are the energy minima of the initial and the final valley, respectively.

The numerical values of the coupling constants and phonon energies for this type of scattering are shown in Table 2.3.

Table 2.3: *Numerical values for the non-equivalent intervalley scattering rate.*

	Silicon	Germanium
D_{GX}	0.0 eV/cm	10^9 eV/cm
$\hbar\omega_{GX}$	0.0 eV	0.02756 eV
D_{GL}	0.0 eV/cm	2.0×10^8 eV/cm
$\hbar\omega_{GL}$	0.0 eV	0.02756 eV
D_{XL}	4.65×10^8 eV/cm	4.1×10^8 eV/cm
$\hbar\omega_{XL}$	0.02283 eV	0.02756 eV

2.5 Intravalley Scattering by Acoustic Phonons

This type of scattering assumes that the initial and final states of an electron are within the same valley. The acoustic scattering mechanism is assumed to be elastic which is an approximation called equipartition. For this type of scattering the transition probability is given by:

$$\lambda(\epsilon) = \frac{2\pi k_B T_L D_{Ai}^2}{\hbar u_s^2 \rho} g_i(\epsilon) \qquad \text{.....(1.21)}$$

where i is the valley index, T_L is the lattice temperature, D_{Ai} is the acoustic deformation potential of the i-th valley, u_s denotes the average sound velocity, ρ is the density of the crystal and $g_i(E)$ the density of states per spin in the i-th valley which is defined by the following formula:

$$g_i(\epsilon) = \frac{1}{(2\pi)^3} \int_{BZ} \delta(\epsilon - \epsilon_i(\boldsymbol{k}))d^2k \qquad \text{.....(1.22)}$$

For the analytical band structure, it follows from :

$$g_i(\epsilon) = \frac{1}{(2\pi)^3} \frac{2m_{di}^*}{\hbar^2} \sqrt{\gamma_i(\epsilon)}(1 + 2\alpha_i\epsilon) \qquad \text{.....(1.23)}$$

where m_{di}^{*} is the density of states effective mass for the i[th] valley, and $\gamma_i(E)$ denotes the band-form function [14]:

$$\gamma_i(\epsilon) = \epsilon(1 + \alpha\epsilon_i) \qquad \text{.....(1.24)}$$

The average sound velocity is defined as:

$$u_s = \frac{1}{3}(2u_t + u_i) \qquad \text{..... (1.25)}$$

Where u_t and u_i are the transverse and longitudinal components of the sound velocity. The numerical values for the parameters of the acoustic phonon scattering rate are given in table 2.4.

Table 2.4: *Numerical values for the acoustic phonon scattering rate*

	D_{A_X}	D_{A_L}	ρ	u_t	u_l
Silicon	7.2 eV	11.0 eV	2.338×10^{-3} kg/cm^3	5.410×10^5 cm/sec	9.033×10^5 cm/sec
Germanium	9.58 eV	8.84 eV	5.32×10^{-3} kg/cm^3	3.61×10^5 cm/sec	5.31×10^5 cm/sec

2.6 Summery of Scattering in Pure Silicon

For intrinsic silicon the effects of electron-electron, and impurity scattering need not be included, so important scattering governed by, long wave length (low energy) acoustic phonons, which called intravalley phonons, and short wave length (high energy) intervalley phonons. in principle, whenever electron interact with phonon a definite energy absorbed or emitted by the scattered electron disregarding on the type of phonon, however, in order to simplify the calculations; collisions treated as elastic processing if the absorbed (or emitted) energy is negligible compression to electron's energy. The associated energy for intravalley acoustic phonon is very low so the process can be approximate as

elastic such that the final electron state falls in the same valley, while the associated energy with intervalley phonons high, and comparable to electron's kinetic energy, hence the interaction is inelastic. The momentum conservation ascertains if final electron state falls in other valley for intervalley scattering in silicon. As referred earlier, silicon has six equivalent valleys which illustrated in figure 2.5. The associated intervalley phonons called equivalent intervalley phonons. The electron's transition within these valleys classified into two types: The first, *g-type* , which related to electron transient between parallel valleys, for example $< 100 > \rightarrow < \bar{1}00 >$, and so on . For such transition there is only one choice for the final valley. The second one is *f-type*, this is happened between perpendicular valleys, for example $< 100 > \rightarrow < 010 >, < 0\bar{1}0 >, < 00\bar{1} >$. Hence, there are four choices for the final valleys among each *f-type* transition. The *f-type*, and *g-type* transitions illustrated schematically in figure 1.2.The important parameter for each of these six modes $(f_1, f_2, f_3, g_1, g_2, g_3)$, are: associated phonons energy, and deformation coupling potential energy. For present work these parameters, which listed in table 1.6, are fixed during calculations. These parameters as well as the material constants are similar to those which have been used in for Monte Carlo simulation [15] which Used in Present calculations and listed in table

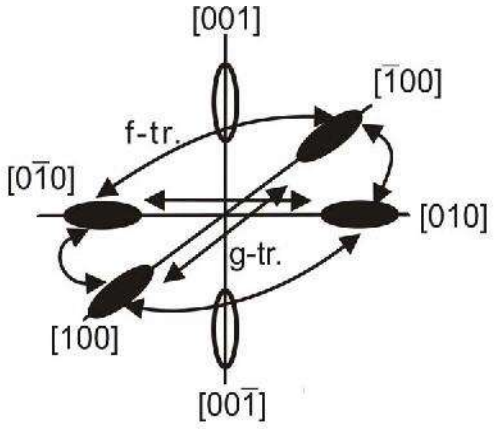

Figure 2.2: *Description of f-type, and g-type processes for silicon's ellipsoidal equal energy.*

Table 2.4 : Set of Physical Parameters for Silicon Used in Present calculations [15]

Name	Symbol	Value	Unit
$f_1(TA)$: equivalent energy, coupling constant	$\hbar\omega_{f1}$ D_{f1}	0.019 0.3×10^{10}	eV eV/m
$f_2(LA)$: equivalent energy coupling constant	$\hbar\omega_{f2}$ D_{f2}	0.047 2×10^{10}	eV eV/m
$f_3(TO)$: equivalent energy coupling constant	$\hbar\omega_{f3}$ D_{f3}	0.059 2×10^{10}	eV eV/m
$g_1(TA)$: equivalent energy coupling constant	$\hbar\omega_{g1}$ D_{g1}	0.012 0.5×10^{10}	eV eV/m
$g_2(LA)$: equivalent energy coupling constant	$\hbar\omega_{g2}$ D_{g2}	0.018 0.8×10^{10}	eV eV/m
$g_3(LO)$: equivalent energy coupling constant	$\hbar\omega_{g3}$ D_{g3}	0.062 11×10^{10}	eV eV/m
Acoustic deformation potential	D_{ac}	9.0	eV
Free electron mass	m_0	9.1093897×10^{-31}	kg
Longitudinal effective mass	m_l	$0.98m_0$	kg
Transverse effective mass	m_t	$0.19m_0$	kg
Longitudinal sound velocity	u_l	9×10^5	m/s
Transverse sound velocity	u_t	5.3×10^5	m/s
Crystal density	ρ	2330	kg/m^3
Non-parabolicity factor	α	0.5	eV^{-1}

Chapter three

Results and discussion

For present work, both acoustic, and the intervalley scattering taken into account for silicon's nonparabolicity /ellipsoidal energy surface.

The scattering with crystal vibrations in the acoustic mode is taken into account in the elastic approximation, while the intervalley phonon interactions is considered in the inelastic approximation, and thus the emission, and absorption of phonons of energy $\hbar\omega_j$, where $j = (1,2,\ldots\ldots,15)$, are considered .The following formulas have been used in recent study which also reviewed in detailed studies[15, 16]. The basic theory reviewed in [7] and references therein.

1. For acoustic(intravalley) phonons the scattering rate $\frac{1}{\tau_{ac}}$ as a function of electron energy is given by [14]:

$$\frac{1}{\tau_{ac}(\varepsilon)} = \frac{2^{1/2} D^2_{ac}\, m_D^{3/2} k_B T}{\pi\, \hbar^4 u_S^2 \rho} \gamma(\varepsilon)^{1/2}\ \gamma'(\varepsilon) \qquad (3.1)$$

Where $\gamma(\varepsilon)$, is given by equation (1.5), $\gamma'(\varepsilon)$ is the first derivative of $\gamma(\varepsilon)$ respect to energy, ρ, is material concentration, u_s, is the average velocity of sound in the crystal, where $u_s = \frac{1}{3}(2u_t + u_l)$, where u_t, , and u_l, are the transverse, and longitude components of sound velocity [15].

Equation (3.1) also valued for intermediate models such as: spherical /nonparabolic, where $m_l = m_t$, and $u_s = u_l$, or ellipsoidal /parabolic, where the nonparabolicity factor $\alpha = 0$.

2. For one type intervalley phonons, since there are 15 probabilities, the scattering rate $\frac{1}{\tau_{iv}}$ as a function of electron energy is given by [17] :

$$\frac{1}{\tau_{iv}(\varepsilon)} = \frac{D_{iv}^2\, m_D^{3/2}}{2^{1/2}\pi\,\hbar^3\rho\, w_{iv}}\left[\frac{1}{e^{\hbar\omega/k_BT}-1}\right]\left[\begin{array}{l}\gamma^{1/2}(\varepsilon+\hbar\omega)\dfrac{d\gamma(\varepsilon+\hbar\omega)}{d\gamma}+\\ e^{\hbar\omega/k_BT_L}\;\gamma^{1/2}(\varepsilon-\hbar\omega)\dfrac{d\gamma(\varepsilon-\hbar\omega)}{d\gamma}\end{array}\right]$$

…… (3.2)

Where the parameters D_{iv} , ρ, ω are intervalley coupling, crystal density, phonon vibration frequency, respectively, and the functions

$$\gamma^{1/2}(\varepsilon \pm \hbar\omega) = \left(\frac{\partial\gamma(\varepsilon \pm \hbar\omega)}{\partial\varepsilon}\right)^{1/2} \qquad (3.3)$$

Where $(\varepsilon \pm \hbar\omega)$ is final electron energy, and the minus (or plus) sign refer to phonon emission (or absorption) as referred previously. Combination the acoustic, and intervalley scattering rates, hence the total scattering rate for acoustic, and one type of intervalley phonon becomes [14,17]

$$\frac{1}{\tau} = \frac{1}{\tau_{ac}} + \frac{1}{\tau_{iv}} \qquad \ldots\ldots\ldots\ldots\ldots\ldots\ldots\ldots\ldots\ldots \qquad (3.4)$$

Including all intervalley phonons in silicon, hence (3.4) can be written as

$$\frac{1}{\tau} = \frac{1}{\tau_{ac}} + \sum_{j=1}^{15}\frac{1}{\tau^{(j)}{}_{iv}} \qquad \ldots\ldots\ldots\ldots\ldots\ldots \qquad (3.5)$$

Where the sum takes over all possible transition through the six valleys of silicon. The last equation applied for calculation of Total Scattering Rate (TSR) in present work. the calculation for TSR is based on coupling constants, and other parameters which listed in table 2.4.

A MATLAB program has also been written to calculate equation (3.5), which can be found in the appendix.

According to equations (3.1), and (3.2), the total scattering rate $\frac{1}{\tau(\varepsilon)}$, explicitly proportional with the density of final states that given by (3.5), hence one can express that rate as a parameter multiplied by density of state

$$\frac{1}{\tau(\varepsilon)} = \frac{1}{\tau_0}\gamma^{1/2}(\varepsilon)\gamma'(\varepsilon) \qquad \ldots\ldots \qquad (3.6)$$

The total scattering rate $\frac{1}{\tau(\varepsilon)}$ is given by equation (3.5).

Figure 3.1 illustrate the variation of total scattering rate with electron energy in first conduction band of silicon . It is noted that the scattering rate increase as electron energy increase because the increasing of density of state and the total electron–phonon scattering rate increases strongly with temperature . similar results are founded in lectures [18, 19], while optical phonons dominate the total electron–phonon scattering rate at 300 and 77 K, and the main contribution to the energy loss rate comes from optical modes which are inelastic.The calculated values of scattering rate at band edge are $1.2 \times 10^{14} s^{-1}$ and $3.1 \times 10^{13} s^{-1}$ at $300k$ and $77k$, respectively.

The parameter $\frac{1}{\tau_0}$ in equation (3.6) can be calculated by plotting $\frac{1}{\tau(\varepsilon)}$, vs. $\gamma^{1/2}(\varepsilon)\gamma'(\varepsilon)$, hence τ_0, represent the inverse of the slope. Appling this method, the calculated values for τ_0 in this calculation are:

$$\tau_0 = \begin{bmatrix} 4.07\times10^{-14}\, eV^{1/2}\, s & for\ \varepsilon < 0.062\ eV \\ 1.98\times10^{-14}\ eV^{1/2}\, s & for\ \varepsilon > 0.062\ eV \end{bmatrix} \qquad \ldots. \qquad (3.7)$$

When lattice temperature is $300k$.

While for lattice temperature $77k$, the obtained values for τ_0, are:

$$\tau_0 = \begin{bmatrix} 19\times10^{-14}\, eV^{1/2}\, s & for\ \varepsilon < 0.028\ eV \\ 3.43\times10^{-14}\ eV^{1/2}\ s & for\ \varepsilon > 0.028\ eV \end{bmatrix} \quad \text{.....} \quad (3.8)$$

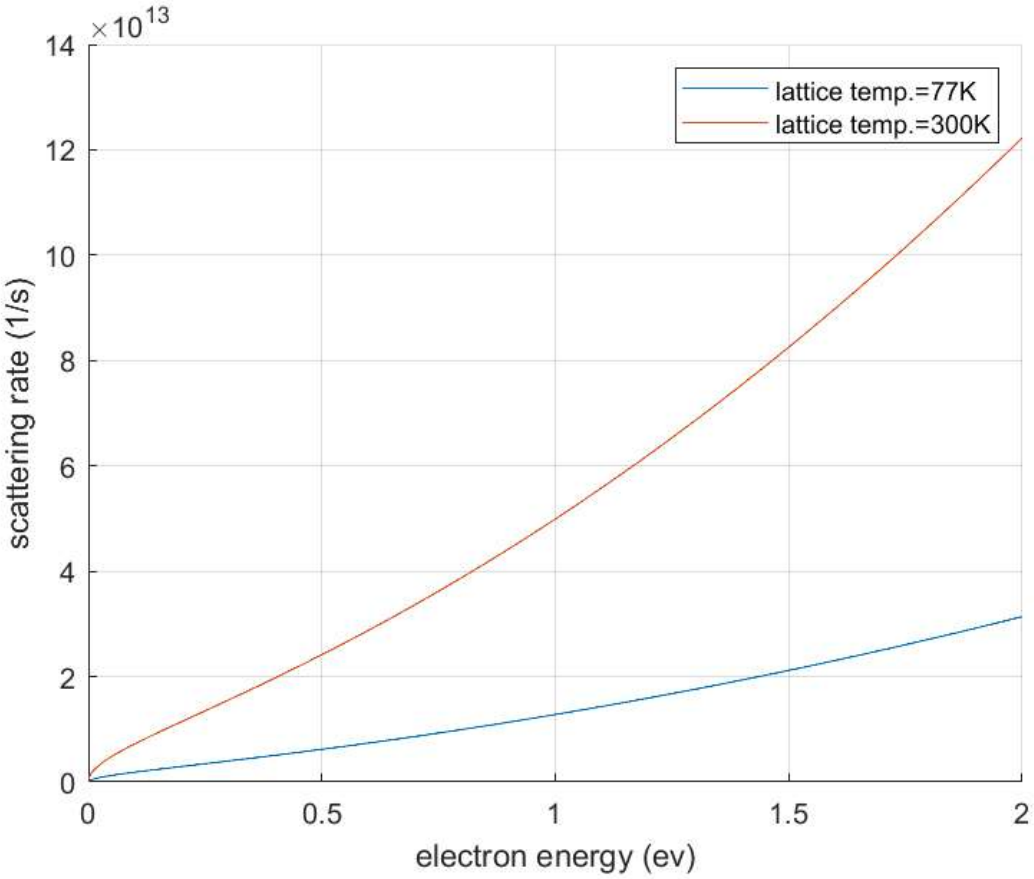

Figure 3.1 : Total scattering rate of the first conduction band of silicon at 77 and 300K including multi sub bands, acoustic and optical phones.

Conclusions

We successfully modeled the electron -phonon interaction in silicon via calculating the total scattering rate which is the inverse of relaxation time between electron-phonon collision . The multi sub band, intervalley and intravalley phonons and ellipsoidal energy surfaces of first conduction band of silicon are included in this model. A suitable MATLAB software have been bullied to maintain the calculations.

Reference

[1] Guzmán-Verri, G.G. and Voon, L.L.Y., 2007. Electronic structure of silicon-based nanostructures. Physical Review B, 76(7), p.075131.

[2] Cerasoli, F.T., Sherbert, K., Sławińska, J. and Nardelli, M.B., 2020. Quantum computation of silicon electronic band structure. Physical Chemistry Chemical Physics, 22(38), pp.21816-21822

[3] Gonzalez-Zalba, M.F., de Franceschi, S., Charbon, E., Meunier, T., Vinet, M. and Dzurak, A.S., 2021. Scaling silicon-based quantum computing using CMOS technology. Nature Electronics, 4(12), pp.872-884.

[4] Ahmed, M.J., 2017, September. Temperature dependence of electron impact ionization coefficient in bulk silicon. In AIP Conference Proceedings (Vol. 1888, No. 1, p. 020034). AIP Publishing LLC.

[5] Anile, A.M., Russo, G. and Romano, V., 2000. Extended hydrodynamical model of carrier transport in semiconductors. SIAM Journal on Applied Mathematics, 61(1), pp.74-101.

[6] Fang, T., Konar, A., Xing, H. and Jena, D., 2011. High-field transport in two-dimensional graphene. Physical Review B, 84(12), p.125450.

[7] Lundstrom, M., 2002. Fundamentals of carrier transport, 2nd edn. Measurement Science and Technology, 13(2), pp.230-230.

[8] Kittel, C. and McEuen, P., 2018. Introduction to solid state physics. John Wiley & Sons.

[9] Dhar, S., 2007. Analytical mobility modeling for strained silicon-based devices. TU Wien.

[10] Hearn, C.J., 1965. Inter-carrier energy exchange and the critical concentration of hot carriers in a semiconductor. Proceedings of the Physical Society (1958-1967), 86(4), p.881.

[11] Wessner, W., 2006. Mesh refinement techniques for TCAD Tools (Doctoral dissertation).

[12] Peter, Y.U. and Cardona, M., 2010. Fundamentals of semiconductors: physics and materials properties. Springer Science & Business Media

[13] Smirnov, S., 2003. Physical modeling of electron transport in strained silicon and silicon-germanium (Doctoral dissertation).

[14] Goldsman, N., Henrickson, L. and Frey, J., 1991. A physics-based analytical/numerical solution to the Boltzmann transport equation for use in device simulation. Solid-state electronics, 34(4), pp.389-396.

[15] Jacoboni, C. and Reggiani, L., 1983. The Monte Carlo method for the solution of charge transport in semiconductors with applications to covalent materials. Reviews of modern Physics, 55(3), p.645.

[16] Wu, Y.J. and Goldsman, N., 1993. AN EFFICIENT SOLUTION OF THE MULTI-BAND BOLTZMANN TRANSPORT EQUATION IN SILICON. COMPEL-The international journal for computation and mathematics in electrical and electronic engineering.

[17] Wu, Y.J. and Goldsman, N., 1993. AN EFFICIENT SOLUTION OF THE MULTI-BAND BOLTZMANN TRANSPORT EQUATION IN SILICON. COMPEL-The international journal for computation and mathematics in electrical and electronic engineering.

[18] Sen, R., Vast, N. and Sjakste, J., 2022. Hot electron relaxation and energy loss rate in silicon: Temperature dependence and main scattering channels. Applied Physics Letters, 120(8), p.082101.

[19] Sen, R., Vast, N. and Sjakste, J., 2022, May. Photoexcited electron dynamics and energy loss rate in silicon: temperature dependence and main scattering channels. In Advances in Ultrafast Condensed Phase Physics III (Vol. 12132, pp. 7-13). SPIE.

Appendix
MATLAB script file for scattering rate calculations

```
clc
format short
for kk=1:2
    switch kk
     case 1
TL=77                          % lattice temp
e_gap=1.17; % energy gap of silicon at 77k

case 2

TL=300 ;                        % lattice temp
e_gap=1.12                     % energy gap of silicon  at 300k
    end

eg=(e_gap*1000);
egc=round(eg*1.5)
n=2000;
e=0;
dxi=zeros(1,15);
k23i=zeros(1,15);
k32i=zeros(1,15);
k22i=zeros(1,15);
k33i=zeros(1,15);
hd1=zeros(1,n);
t2=zeros(1,n);
t3=zeros(1,n);
E=zeros(1,n);
tot=zeros(1,n);
ech=1.60217733e-19;            % electron charge
Ej=zeros(1,n);
format short e
% M=zeros(1,n);
e=0; h=0.001;
m0=9.1093897e-31;             % free electron mass
b=0.5;
mt=.19*m0;                     % transverse electron mass
ml=.98*m0;                     % longitudnal electron mass
roo=2330;
dac=9.0;                       % deformation potential of acousic
phonon
hb=6.582122025e-16;
kt=(TL/300)*0.02585215;
```

```
hbwi=1e-3*[12 18 19 19 19 19 47 47 47 47 58 58 58 58 61 ];   %
phonon freq.  see table 2.1
wi=hbwi./hb;
di=1e10*[ 0.5 0.8 0.3 0.3 0.3 0.3 2 2 2 2 2 2 2 2 11];  %
deformation potntal ev/m  , see table 2.1
di=0;
 ds=di.^2./wi;                                                %
square deformation/w  , equation (2.17)
ut=5.34e3;                                                  %
transverse component of sound velocity
ul=9.04e3;                                      % longitude
component of sound velocity
us=(2*ut+ul)/3;                  % sound velocity

zac=2^0.5*dac^2*(mt^2*ml)^0.5*kt/(pi*hb^4*roo* us^2);      %
acoustic Parameter
ziv=(mt^2*ml)^0.5*ds./(2^0.5*pi*hb^3*roo);                  %
intervally  Parameter
pri=hbwi./kt;
p1i=exp(pri);      % exp(hw/kt)
mi=1./(p1i-1);    %  phonon occupation number
Nq=1/(exp(hw/kt)-1) , see equation (2.11)

for j=1:n
e=e+h;
E(j)=e;



k2=e+b*e^2;     % gamma energy dispersion law gama(e),  see
equatoin (2.3)
k3=1+2*b*e;     % 1 st derivitive of gama(e)=gama' , see
equations 2.9 , 2.17 , 2.18

k5=k2^0.5;      %  =gama^0.5


 hd1(j)=k5.*k3 ; % density of state =gamma^.5 x gamma' , see
equation 2.9



k22i=(e+hbwi)+b*(e+hbwi).^2 ;  % gamma at (e+hw)
k32i=1+2*b*(e+hbwi);           % gamma' at (e+hw)

% transform the energy to vector matrix
on=ones(1,15);
ei=e*on;

dxi=ei-hbwi ;  % the differnce between the enrgy and
intervally phonnon energy
```

```
k23i=dxi+b*dxi.^2;                  % gamma(e-hw)
k33i=1+2*b*dxi;                     % gamma'(e-hw)
     for i =1:15                   % see equation 2.20b
         if dxi(i)<0
            k23i(i)=0;
            k33i(i)=0;
          end
      end


aai=k22i.^0.5.*k32i;              % gamma(e+hw)^0.5 *gamma'(e+hw)
hhi=k23i.^0.5.*k33i;              % gamma(e-hw)^0.5 *gamma'(e-hw)
t1(j)=zac*hd1(j);
t2(j)=sum(ziv.*mi.*(aai+p1i.*hhi));
t3(j)=t1(j)+t2(j);
% t3(j)=t3(j)/sqrt(ech);
sca_rate(j)=hd1(j)/t3(j);
end

tp1=t3(eg);
tp2=t3(egc);
grid on
hold on
% plot(hd1,t3/sqrt(ech))
plot(E,t3/sqrt(ech))
xlabel('electron energy (ev)')
ylabel('scattering rate (1/s)' )
legend ('lattice temp.=77K','lattice temp.=300K')
end
```